REPORT DOCUMENTATION PAGE

1. REPORT DATE *(DD-MM-YYYY)*	2. REPORT TYPE	3. DATES COVERED *(From - To)*
08-02-2005	Journal Article (refereed)	

4. TITLE AND SUBTITLE

Wave Number Spectrum and Mean Square Slope of Intermediate-scale Ocean Surface Waves

5a. CONTRACT NUMBER

5b. GRANT NUMBER

5c. PROGRAM ELEMENT NUMBER
PE061153 and 062435

6. AUTHOR(S)

Hwang, Paul A.

5d. PROJECT NUMBER

5e. TASK NUMBER

5f. WORK UNIT NUMBER
73-6628-A5-5

7. PERFORMING ORGANIZATION NAME(S) AND ADDRESS(ES)

Naval Research Laboratory
Oceanography Division
Stennis Space Center, MS 39529-5004

8. PERFORMING ORGANIZATION REPORT NUMBER

NRL/JA/7330-05-5199

9. SPONSORING/MONITORING AGENCY NAME(S) AND ADDRESS(ES)

Office of Naval Research
800 N. Quincy St.
Arlington, VA 22217-5660

10. SPONSOR/MONITOR'S ACRONYM(S)

ONR

11. SPONSOR/MONITOR'S REPORT

12. DISTRIBUTION/AVAILABILITY STATEMENT

Approved for public release, distribution is unlimited

20060605031

13. SUPPLEMENTARY NOTES *U.S. Government author: Hwang. U.S. Govt work; not copyrighted.*

14. ABSTRACT

This paper presents an analysis of the wave number spectra of intermediate-scale waves (wavelengths between 0.02 and 6 m) covering a wide range of wind and background wave conditions under various sea-state conditions. The main result of the analysis is that the dependence of the dimensionless wave spectrum on the dimensionless wind friction velocity follows a power law function. The coefficient and exponent of the power law function vary systematically with the wave number. The wave number dependence of the coefficient and exponent serves as an empirical parameterization for computing the wave number spectra of intermediate-scale waves at different wind speeds. Calculation of the mean square slope from the resulting wave number spectrum confirms that intermediate-scale waves are the dominant contributor of the ocean surface roughness. A simple formula is presented for calculating the band-pass filtered mean square slope of the ocean surface for remote sensing applications.

15. SUBJECT TERMS

wave number spectra, intermediate-scale waves, parameterization function, mean square

16. SECURITY CLASSIFICATION OF:			17. LIMITATION OF ABSTRACT	18. NUMBER OF PAGES	19a. NAME OF RESPONSIBLE PERSON
a. REPORT	b. ABSTRACT	c. THIS PAGE	UL	7	Paul Hwang
Unclassified	Unclassified	Unclassified			19b. TELEPHONE NUMBER *(Include area code)* (202) 404-0800

PUBLICATION OR PRESENTATION RELEASE REQUEST

Pubkey: 4464   NRLINST 5600.2

1. REFERENCES AND ENCLOSURES	2. TYPE OF PUBLICATION OR PRESENTATION	3. ADMINISTRATIVE INFORMATION

1. REFERENCES AND ENCLOSURES

Ref: (a) NRL Instruction 5600.2
(b) NRL Instruction 5510.40D

Encl: (1) Two copies of subject paper
(or abstract)

2. TYPE OF PUBLICATION OR PRESENTATION

( ) Abstract only, published   ( ) Abstract only, not published
( ) Book   ( ) Book chapter
( ) Conference Proceedings   ( ) Conference Proceedings
    (refereed)   (not refereed)
( ) Invited speaker   ( ) Multimedia report
(X) Journal article (refereed)   ( ) Journal article (not refereed)
( ) Oral Presentation, published   ( ) Oral Presentation, not published
( ) Other, explain

3. ADMINISTRATIVE INFORMATION

STRN NRL/JA/7330-05-5199
Route Sheet No. 7330/
Job Order No. 73-6628-A5-5
Classification __X__ U ____ C
Sponsor ONR BASE
approval obtained __X__ yes ____ no

4. AUTHOR

Title of Paper or Presentation
Wavenumber Spectrum and Mean-square Slope of Intermediate-scale Ocean Surface Waves

Author(s) Name(s) (*First,MI,Last), Code, Affiliation if not NRL*

Paul A. Hwang

It is intended to offer this paper to the _____
<div align="center">(Name of Conference)</div>

<div align="center">(Date, Place and Classification of Conference)</div>

and/or for publication in **Journal of Geophysical Research, Unclassified** _____
<div align="center">(Name and Classification of Publication)   (Name of Publisher)</div>

After presentation or publication, pertinent publication/presentation data will be entered in the publications data base, in accordance with reference (a).
It is the opinion of the author that the subject paper (is ____) (is not __X__) classified, in accordance with reference (b).
This paper does not violate any disclosure of trade secrets or suggestions of outside individuals or concerns which have been communicated to the Laboratory in confidence. This paper (does ____) (does not __X__) contain any militarily critical technology.
This subject paper (has ____) (has never __X__) been incorporated in an official NRL Report.

_____
Paul A. Hwang, 7332
Name and Code (*Principal Author*)   (Signature)

5. ROUTING/APPROVAL

CODE	SIGNATURE	DATE	COMMENTS
Author(s) Hwang	*Paul A Hwang*	4/13/05	*Need by 10 may 05*
			Publicly accessible sources used for this publication
Section Head Hwang	*Paul A Hwang*	4/13/05	
Branch Head **Robert A Arnone, 7330**	*John C Kindle*	4/14/05	
Division Head **Ruth H. Preller, 7300**		4/14/05	1. Release of this paper is approved. 2. To the best knowledge of this Division, the subject matter of this paper (has ____) (has never __X__) been classified.
Security, Code **7030.1**		4/20/05	1. Paper or abstract was released. 2. A copy is filed in this office SCC-186-5
Office of Counsel,Code **1008.3**		4/19/05	
ADOR/Director NCST **E.O. Hartwig, 7000**			
Public Affairs (*Unclassified/ Unlimited Only*), Code **7030.4**	*Becky Roland*	4/18/05	
Division, Code			
Author, Code			

HQ-NRL 5511/6 (Rev. 12-98) (e)   THIS FORM CANCELS AND SUPERSEDES ALL PREVIOUS VERSIONS

Wave number spectrum and mean square slope of intermediate-scale ocean surface waves

Paul A. Hwang

Oceanography Division, Naval Research Laboratory, Stennis Space Center, Mississippi, USA

[1] This paper presents an analysis of the wave number spectra of intermediate-scale waves (wavelengths between 0.02 and 6 m) covering a wide range of wind and background wave conditions under various sea-state conditions. The main result of the analysis is that the dependence of the dimensionless wave spectrum on the dimensionless wind friction velocity follows a power law function. The coefficient and exponent of the power law function vary systematically with the wave number. The wave number dependence of the coefficient and exponent serves as an empirical parameterization for computing the wave number spectra of intermediate-scale waves at different wind speeds. Calculation of the mean square slope from the resulting wave number spectrum confirms that intermediate-scale waves are the dominant contributor of the ocean surface roughness. A simple formula is presented for calculating the band-pass filtered mean square slope of the ocean surface for remote sensing applications.

1. Introduction

[2] Surface waves a few centimeters to a few meters long (referred to as the intermediate-scale waves hereafter) are generally believed to be the dominant contributor of the ocean surface roughness. Owing to the large Doppler frequency shift when traditional point-measurement systems are employed, the measurement accuracy of intermediate-scale waves in the ocean is difficult to assess. So far, reliable measurements of intermediate-scale waves in the ocean environment are essentially nonexistent. As a result, verification of the assumption regarding intermediate-scale waves and the ocean surface roughness based on field data is not yet presented. Most ocean wave data focus on the energy-containing frequency band in the neighborhood of the spectral peak of the sea surface displacement. A small fraction of the wave data focuses on the length scale of gravity-capillary waves, using mainly optical scanning sensors to conduct spatial measurements to avoid the tricky problems associated with the Doppler frequency shift [e.g., Hwang et al., 1996; Hara et al., 1998]. Extending the optical scanning techniques to wave components several meters long for field applications is prohibitively expensive and impractical. Hwang et al. [1996] suggested that the problem of Doppler frequency shift can be alleviated by using a free-drifting measurement technique. The effectiveness of removing Doppler frequency shift by free-drifting operations was demonstrated by comparing the wave number-frequency spectra measured by linear arrays of wire gauges deployed in free-drifting and fixed-station configurations [Hwang and Wang, 2004] and reliable conversion

of the wave spectrum from frequency to wave number domain can be extended into intermediate-scale wave components. A more quantitative discussion of the Doppler frequency shift is given in Appendix A.

[3] Hwang and Wang [2004] presented an analysis of field measurements of intermediate-scale waves. Following the suggestion by Phillips [1984], the data were processed to investigate the empirical functional dependence of the dimensionless spectrum, $B(k)$, on the dimensionless wind friction velocity, u_*/c, where k is the wave number and c is the wave phase speed. The result shows that $B(k)$ can be expressed as a power law function of u_*/c. The coefficient and exponent of the power law function are wave number dependent. In this paper, using the above result serving as an empirical parameterization function, the wave number spectra of intermediate-scale waves at different wind speeds are quantified (section 2). The properties of the mean square slopes integrated over different wave number ranges are investigated in section 3. A summary is given in section 4.

2. Empirical Parameterization

[4] In a discussion of the source function balance of short ocean surface waves that are important to remote sensing applications, Phillips [1984] emphasized that the knowledge on the variation of the wave number spectrum with wind speed can provide valuable information on the properties of the dissipation function. Hwang and Wang [2004] reported an analysis of the wave spectra collected in the ocean using a free-drifting technique. The spectra are divided into two different groups: wind seas and mixed seas. The range of wind speeds is 3.6 to 14.2 m/s for the former group (291 cases), and 2.6 to 10.2 m/s for the latter group (106 cases). For each wave component, the scatterplot of $B(k)$ as a
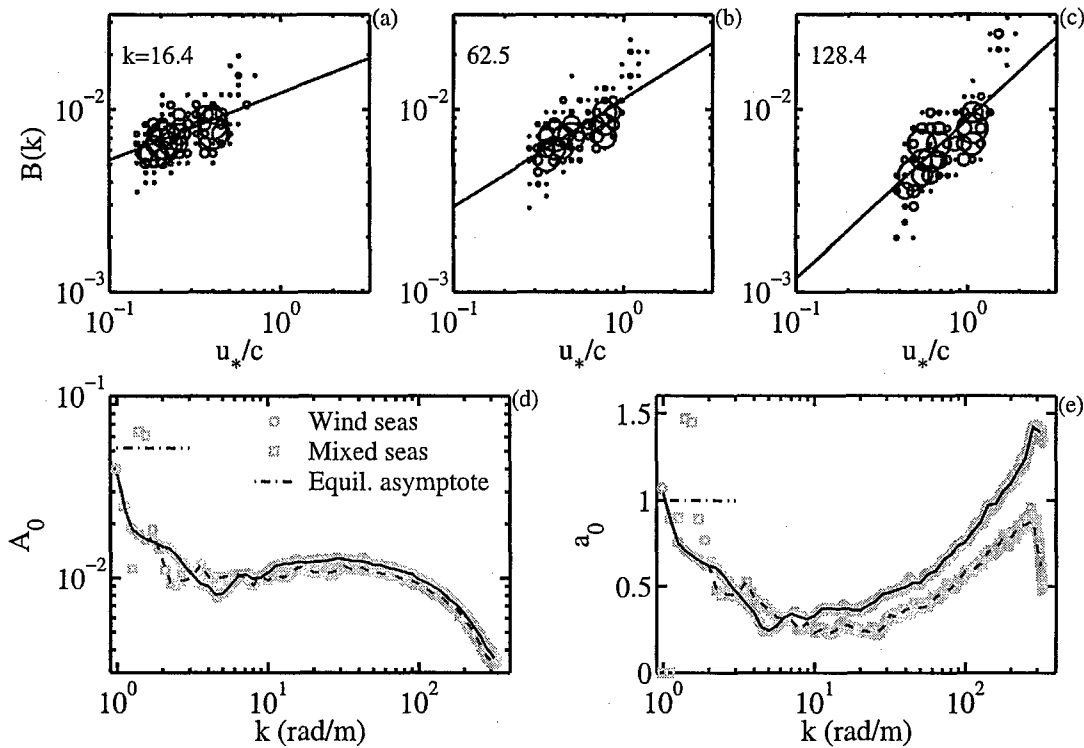
Figure 1. (a)–(c) Examples of the scatterplot of $B(u_*/c)$ for a given wave number component, showing a power law dependence. The wave number is marked at the upper left corner of each panel. The size of the plotting symbol is proportional to the data density at the plotting coordinates. (d) A_0 and (e) a_0 of the power law function derived from least squares fitting of field data. See color version of this figure in the HTML.

function of u_*/c shows a general power law dependence, as illustrated by the examples shown in Figures 1a–1c,

$$B\left(\frac{u_*}{c};k\right) = A_0(k)\left(\frac{u_*}{c}\right)^{a_0(k)}.$$ (1)

The coefficient and exponent of the power law function for each wave component can be calculated from least squares fitting of the ocean data. The variations of A_0 and a_0 with k are depicted in Figures 1d and 1e, respectively. *Hwang and Wang* [2004] presented fifth-order polynomial fitting functions for A_0 and a_0 but the polynomial functions obviously missed many fine features of the variations (see their Figure 3). Here the computation is carried out by using a lookup table interpolating through the measured data (Table 1), the interpolated curves capture most of the subtle details of the variations in A_0 and a_0 (compare the continuous curves and discrete data in Figures 1d–1e). For the range $1 < k < 2$ rad/m, the scatter of the mixed-sea data is large and the wind-sea data in this range are used for both wind seas and mixed seas. The wave number spacing shown in Table 1 is logarithmic. Other interpolation methods such as linear and cubic-spline interpolations in the logarithmic or linear spacing were tested and they produced only small differences in the final construction of A_0 and a_0 curves or the subsequent calculation of $B(k)$ at different wind speeds.

[5] Figure 2 displays the computed wave number spectra over a range of wind speeds using the parameterization

Table 1. Lookup Table of A_0 and a_0 for Wind Seas and Mixed Seas

| k, rad/m	Wind Seas		Mixed Seas	
	$10^3 A_0$	a_0	$10^3 A_0$	a_0
1.00	37.32	1.04	37.32	1.04
1.26	18.60	0.75	18.60	0.75
1.58	16.28	0.67	16.28	0.67
2.00	14.92	0.62	14.92	0.62
2.51	13.09	0.56	13.09	0.56
3.16	10.30	0.45	10.11	0.46
3.98	8.97	0.35	9.98	0.43
5.01	8.21	0.24	10.06	0.36
6.31	10.27	0.32	10.52	0.31
7.94	9.83	0.32	9.08	0.24
10.00	10.71	0.33	9.70	0.23
12.59	11.99	0.37	10.06	0.22
15.85	12.31	0.37	11.50	0.28
19.95	12.24	0.36	10.72	0.24
25.12	12.49	0.41	10.60	0.22
31.62	12.70	0.47	11.63	0.33
39.81	12.38	0.49	11.59	0.36
50.12	11.80	0.52	10.80	0.37
63.10	11.29	0.59	10.42	0.43
79.43	10.82	0.69	9.77	0.49
100.00	9.77	0.76	9.24	0.59
125.89	8.88	0.87	8.13	0.63
158.49	7.58	0.98	7.08	0.71
199.53	6.31	1.10	5.88	0.78
251.19	4.85	1.24	4.36	0.86
316.23	3.61	1.39	3.34	0.62
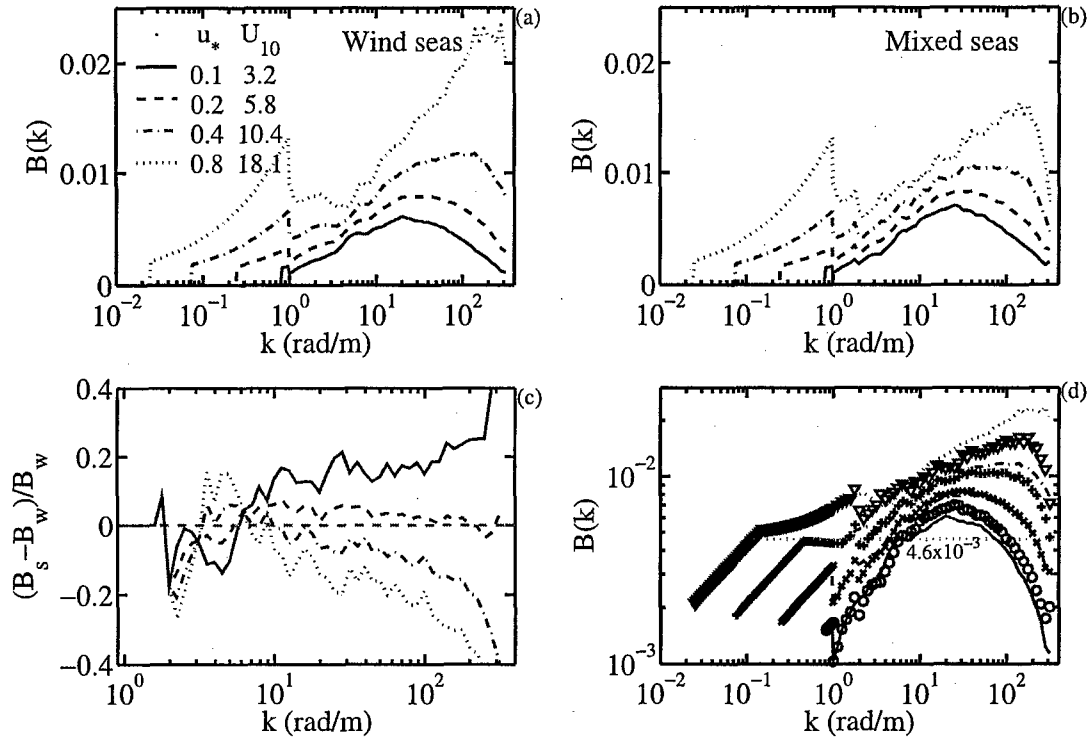
Figure 2. $B(k)$ computed from parameterization function (1) using table lookup for A_0 and a_0 (Table 1): (a) Wind seas and (b) mixed seas plotted in semilogarithmic scales (area conservative representation of the spectrum of mean square slope). (c) The normalized difference of the saturation spectra in wind seas (denoted by subscript w) and mixed seas (denoted by subscript s). (d) $B(k)$, with the kink near $k = 1$ rad/m smoothed, presented in log-log scales. Wind seas are plotted with curves and mixed seas with markers. See color version of this figure in the HTML.

function (1) for the wave number range $1 \leq k \leq 316$ rad/m. The semilogarithmic plots in the top panels represent the area-conservation representation of the mean square slope of the ocean surface; that is, the area under the curve over a range of wave numbers represents the mean square slope of the corresponding spectral wave components, because for the omni-directional spectrum $B(k) = kS_1(k)$, where S_1 is the omni-directional wave slope spectrum (Appendix of *Hwang et al.* [1993]). The results for the wind seas are plotted in Figure 2a and those for the mixed seas in Figure 2b. The normalized spectral difference between the mixed seas and wind seas is shown in Figure 2c. In mixed seas, the background ocean waves modify the spectrum of intermediate-scale waves in a somewhat complex way. For waves shorter than about 1 m, the background waves enhance the spectral densities of intermediate-scale waves at lower wind speeds but reduce their spectral densities at higher wind speeds. For longer intermediate-scale waves, the effect of background waves is opposite to that for the shorter waves. The magnitude of the spectral fluctuations deviating from the wind-sea condition is usually within about 20 percent for most intermediate-scale wave components in the available data. The critical wind speed separating these two opposite trends is somewhat higher than 6 m/s (Figure 2c). Interestingly, the wind speed 7 m/s is frequently associated with the inception of more-intensive breaking events in the ocean and the transition of the surface roughness condition

from smooth or transitional to hydrodynamically rough. The results shown in Figure 2c may reflect the influences of breaking wave and surface roughness conditions on the intermediate-scale waves. The exact effects of wave breaking and roughness conditions on the properties of short- and intermediate-scale waves in the ocean are not well understood. Theoretical investigations on related subjects have indicated that the mechanisms of wave-turbulence interaction and wave breaking exert strong impact on the air-sea momentum transfer and wind-wave generation [e.g., *Makin and Kudryavtsev*, 1999, 2002]. From the empirical data gathered here, it is found that the response of wave components between 1 and 2 m long to the background waves is opposite to that of shorter waves. The data quality of wave components longer than 3 m ($1 < k < 2$ rad/m) in the present dataset is not very good for the mixed-sea conditions, judging from the large data scatter of A_0 and a_0 in this wave number range shown in Figures 1d–1e, and it is difficult to determine the influence of background waves in mixed seas on the longer components of intermediate-scale waves.

[6] For the wave number range $k_p < k < 1$ rad/m, where k_p is the wave number at the peak of the surface displacement spectrum, the equilibrium spectral function is assumed,

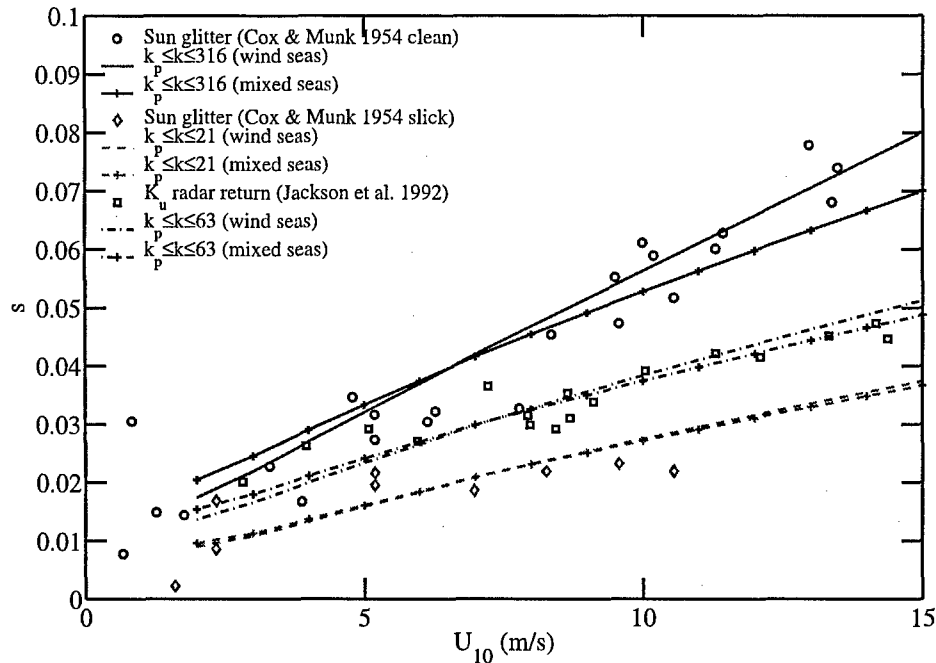$$S_e(k) = bu_* g^{-0.5} k^{-2.5} = b \frac{u_*}{c} k^{-3}, \qquad (2)$$

Figure 3. Mean square slopes integrated from k_p to different upper-bound wave numbers, k_s. Field data from sun glitter and altimeter scattering analyses are also presented for comparison. See color version of this figure in the HTML.

where the spectral constant $b \approx 5.2 \times 10^{-2}$ is used, and g is the gravitational acceleration. The corresponding dimensionless spectrum is

$$B_e(k) = b\left(\frac{u_*}{c}\right). \tag{3}$$

[7] The results shown in Figure 2 illustrate that intermediate-scale waves are the dominant contributor of the ocean surface mean square slope. Numerical integration shows that more than 77 percent of the mean square slope is contributed by waves between 0.02 and 6 m for wind speeds less than 20 m/s. The peak of the mean square slope spectrum represented by $B(k)$ is near 20 rad/m at 3 m/s, and moves toward higher wave number as wind speed increases, reaching to about 200 rad/m at 18 m/s. The dropoff of the spectral densities at the higher wave number end (waves shorter than about 2 cm) is quite steep. There is an apparent kink at $k = 1$ rad/m in merging $B(k)$ and $B_e(k)$, possibly due to the relatively simple equilibrium spectral model used here. This is not considered to be a significant drawback for the discussion of the ocean surface roughness because the contribution of long gravity waves to the overall mean square slope of the ocean surface is relatively small. The kink can be smoothed by interpolation using the spectral data in the neighborhood of $k = 1$ rad/m. A simple linear interpolation is applied to $B(k)$ in the range $6k_p < k < 1.2$ rad/m using values of $B(6k_p)$ and $B(1.2)$. No smoothing is applied if $6k_p \geq 1$ rad/m. Examples of the smoothed spectra are shown in Figure 2d in log-log scales for wind seas and mixed seas together. The smoothing of the spectral kink only introduced a minor change in the mean square slope

computation and does not alter the main conclusions discussed in this paper.

3. Mean Square Slope

[8] Using the wave number spectrum presented in the last section, the mean square slope, s^2, of the ocean surface can be calculated. Because waves longer that the wavelength at the spectral peak make only negligible contribution to the total mean square slope, the lower-bound wave number for integration is set at k_p. The highest wave number of the spectrum considered here is 316 rad/m, thus the mean square slope computed in the following covers almost the full range of the gravity wave spectrum.

[9] The results calculated for the upper-bound cutoff wave numbers of 316, 63, and 21 rad/m (cutoff wavelengths 0.02, 0.1, and 0.3 m) for wind seas and mixed seas are shown in Figure 3. For comparison, field data of the mean square slopes obtained from analyses of sun glitter [*Cox and Munk*, 1954] and airborne K_u-band radar backscattering cross sections [*Jackson et al.*, 1992] are superimposed in the figure. The sun glitter data are further divided into two groups, clean surface and artificial or man-made slicks. The slicks suppress short waves, and the cutoff wave number was estimated to be about 21 rad/m, that is, waves shorter than 0.3 m were suppressed [*Cox and Munk*, 1954]. The agreement between field data and computations appears to be reasonable considering the large data scatter due to difficulties in the acquisition and analysis of such measurements. The sun glitter data in clean-water conditions compare well with the mean square slope integrated from k_p to 316 rad/m, which does not extend into the capillary regime of the wave spectrum. In later theoretical analyses of the
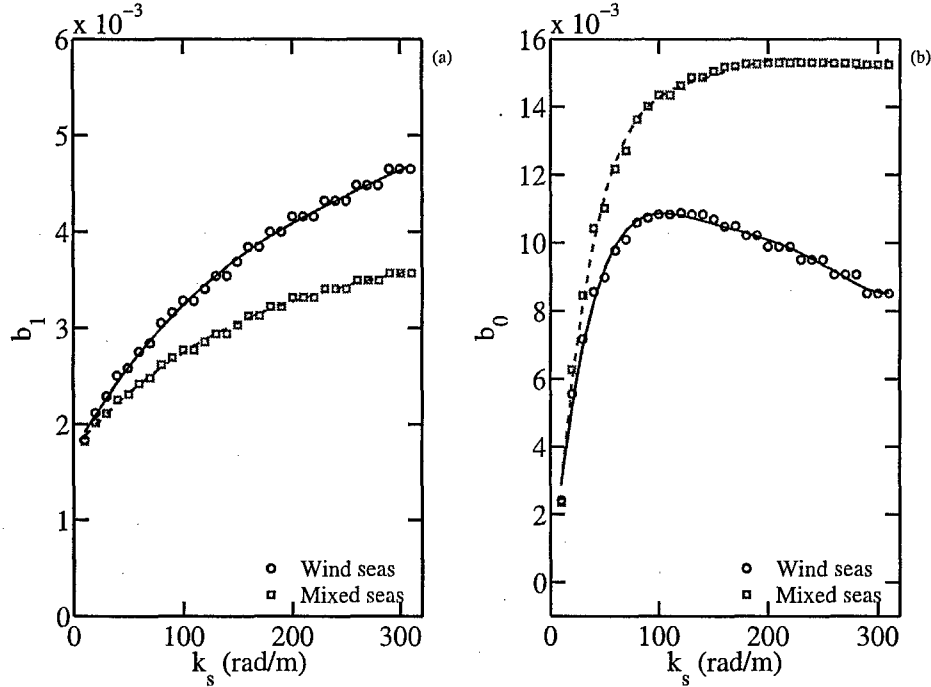
Figure 4. The (a) slope b_1 and (b) intercept b_0 describing the linear wind speed dependence of the mean square slope integrated from k_p to k_s. The polynomial functions of $b_1(k_s)$ and $b_0(k_s)$ for wind seas and mixed seas are given in equation (5) and illustrated as continuous curves in the figure. See color version of this figure in the HTML.

relationship between the surface wave spectrum and the mean square slope [e.g., *Plant*, 1982; *Phillips*, 1985], it has been speculated that capillary waves may not contribute a significant portion to the ocean surface mean square slope but a definitive proof remains unavailable. On the other hand, *Wentz* [1976] evaluated the assumptions used in the data processing of sun glitter by *Cox and Munk* [1954]. He concluded that the contribution from very steep surface slopes cannot be recovered from the mean square slope data derived from the sun glitter measurements as processed by *Cox and Munk* [1954]. Thus the result reported by *Cox and Munk* [1954] only serves to provide a lower bound of the ocean surface mean square slope. The analysis of intermediate-scale waves presented here seems to support the view point expressed by *Wentz* [1976].

[10] *Jackson et al.* [1992] derived the mean square slope of the ocean surface from measurements of the airborne K_u-band altimeter backscattering data. Using their estimation of the diffraction limit of 0.1 m, the mean square slope integrated from k_p to the corresponding wave number

mately linearly with wind speed. The relationship can be written as

$$s^2(k_s) = b_1(k_s)U_{10} + b_0(k_s). \qquad (4)$$

The dependence on k_s of the mean square slope and the coefficients of the linear function of wind speed dependence (slope b_1 and intercept b_0) is written explicitly in equation (4). By varying U_{10} from 2 to 20 m/s in steps of 1 m/s and k_s from 10 to 310 rad/m in steps of 10 rad/m, a dataset of s as a function of U_{10} and k_s is created. Least squares fitting procedure is applied to compute $b_1(k_s)$ and $b_0(k_s)$ for the wind seas and mixed seas (Figure 4). The background waves in mixed seas increase the ambient level of the ocean surface roughness (reflected by b_0) and reduce the rate of increase of surface roughness with wind speed (reflected by b_1). The systematic variations of $b_1(k_s)$ and $b_0(k_s)$ can be represented by the following polynomial functions

$$(5)$$

$$b_1 = \begin{cases} 6.34 \times 10^{-11}k_s^3 - 5.26 \times 10^{-8}k_s^2 + 1.98 \times 10^{-5}k_s + 1.72 \times 10^{-3}, \text{wind seas} \\ 3.72 \times 10^{-11}k_s^3 - 3.43 \times 10^{-8}k_s^2 + 1.30 \times 10^{-5}k_s + 1.75 \times 10^{-3}, \text{mixed seas} \end{cases}$$

$$b_0 = \begin{cases} 5.72 \times 10^{-14}k_s^5 - 5.53 \times 10^{-11}k_s^4 + 2.07 \times 10^{-8}k_s^3 - 3.79 \times 10^{-6}k_s^2 + 3.31 \times 10^{-4}k_s - 1.13 \times 10^{-3}, \text{wind seas} \\ 7.41 \times 10^{-14}k_s^5 - 7.06 \times 10^{-11}k_s^4 + 2.60 \times 10^{-8}k_s^3 - 4.67 \times 10^{-6}k_s^2 + 4.22 \times 10^{-4}k_s - 9.39 \times 10^{-4}, \text{mixed seas} \end{cases}$$

(62.8 rad/s) yields reasonable agreement with their analysis (Figure 3).

[11] Empirically, the mean square slope integrated from k_p to an upper bound wave number, k_s, increases approxi-

Equation (5) can be used to calculate the mean square slopes of arbitrary wave number bands of surface gravity waves. The quantification of the band-pass filtered mean square slopes, such as the tilting and Bragg scattering
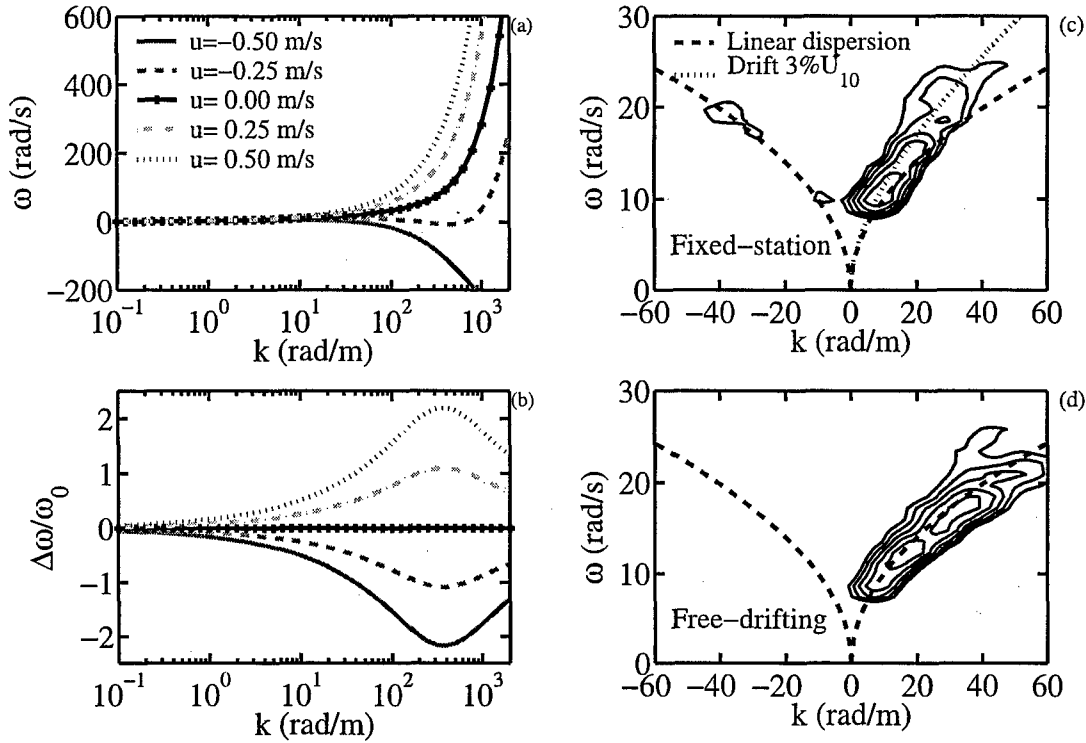
Figure A1. (a) The dispersion relation of surface waves in the presence of background currents. (b) The ratio between the current-induced Doppler frequency shift and the intrinsic wave frequency. Two-dimensional spectra obtained by wave gauge arrays in (c) fixed-station and (d) free-drifting measurements. See color version of this figure in the HTML.

components of the sea surface roughness, are frequently needed in many remote sensing applications such as the computation of the radar scattering cross section and the modulation transfer function [e.g., *Plant*, 1986, 1997].

4. Summary

[12] Field measurements of intermediate-scale waves were obtained using a free-drifting measurement technique to reduce the complication in frequency-to-wave number conversion associated with Doppler frequency shift encountered in fixed-station data. Following an analysis by *Phillips* [1984] on the source function balance of surface waves, the dependence of the dimensionless spectrum, $B(k)$, on the dimensionless wind friction velocity, u_*/c, is investigated. The result shows that $B(u_*/c)$ can be represented by a power law function. The proportionality coefficient, A_0, and the exponent, a_0, of the power law function are determined from field data. The parameterization functions $A_0(k)$ and $a_0(k)$ can then be used to construct the wave number spectra of intermediate-scale waves at different wind speeds (section 2). Using this spectral model, the band-pass filtered mean square slope is derived. The calculated mean square slopes are in good agreement with those obtained from analyses of sun glitter [*Cox and Munk*, 1954] and K_u band altimeter scattering cross sections [*Jackson et al.*, 1992]. Empirically, it is found that the mean square slope integrated from k_p to k_s ($k_s \geq \sim 10$ rad/m) increases approximately linearly with wind speed. For convenient computation of the band-pass filtered ocean surface rough-

ness components frequently needed in remote sensing applications, polynomial functions on the wave number dependence of the slope and intercept of the linear wind speed function are presented as equation (5).

Appendix A: Doppler Frequency Shift

[13] Figure A1a shows the dispersion relation $\omega = \omega_0 + \Delta\omega$, and Figure A1b shows the ratio between the current-induced Doppler frequency shift, $\Delta\omega = u \bullet k$, and the intrinsic frequency, $\omega_0 = (gk + \tau k^3)^{1/2}$, where u is the surface current vector with modulus u, k is the wave number vector with modulus k, and τ is the ratio between the surface tension and the water density. The range of the surface currents used in the computation is from -0.5 to 0.5 m/s, which is a common range of wave-induced orbital velocities in field or laboratory environment. For example, current amplitude of 0.5 m/s can be generated by waves with 6-s wave period and 0.5-m wave amplitude, or 1-s period and 0.08-m wave amplitude. As shown in Figure A1b, the signal from Doppler frequency shift is more than twice the intrinsic value of gravity-capillary waves. The Doppler frequency shift is still quite substantial in the meter-long wave components and amounts to about 40 percent of the intrinsic frequency at ±0.5 m/s current levels. *Hwang et al.* [1996] suggested that the problem of Doppler frequency shift can be considerably reduced by using a free-drifting measurement technique. Experiments were carried out to compare the wave number-frequency spectra, $S(k, \omega)$, measured by linear arrays of wire gauges deployed in free-

drifting and fixed-station configurations in a canal about 100 m wide and 400 m long. With fixed-station measurements, the distribution of $S(k, \omega)$ show the typical shift from the linear dispersion relation (Figure A1c). The magnitude of the net frequency shift is in agreement with that induced by a surface drift current of about two to three percent wind speed. There are also apparent upwind-traveling wave components (negative k and positive ω in Figure A1c). In contrast, the distribution of $S(k, \omega)$ from free-drifting measurements concentrates along the linear dispersion curve and the upwind traveling components disappear (Figure A1d).

References

Cox, C. S., and W. Munk (1954), Statistics of the sea surface derived from sun glitter, *J. Mar. Res.*, *13*, 198–227.

Hara, T., E. J. Bock, J. B. Edson, and W. R. McGillis (1998), Observation of short wind waves in coastal waters, *J. Phys. Oceanogr.*, *28*, 1425–1438.

Hwang, P. A., and D. W. Wang (2004), An empirical investigation of source term balance of small scale surface waves, *Geophys. Res. Lett.*, *31*, L15301, doi:10.1029/2004GL020080.

Hwang, P. A., D. B. Trizna, and J. Wu (1993), Spatial measurements of short wind waves using a scanning slope sensor, *Dyn. Atmos. Oceans*, *20*, 1–23.

Hwang, P. A., S. Atakturk, M. Sletten, and D. B. Trizna (1996), A study of the wavenumber spectra of short water waves in the ocean, *J. Phys. Oceanogr.*, *26*, 1266–1285.

Jackson, F. C., W. T. Walton, D. E. Hines, B. A. Walter, and C. Y. Peng (1992), Sea surface mean-square slope from K_u-band backscatter data, *J. Geophys. Res.*, *97*, 11,411–11,427.

Makin, V. K., and V. N. Kudryavtsev (1999), Coupled sea surface-atmosphere model 1. Wind over waves coupling, *J. Geophys. Res.*, *104*, 7613–7623.

Makin, V. K., and V. N. Kudryavtsev (2002), Impact of dominant waves on sea drag, *Boundary Layer Meteorol.*, *103*, 83–99.

Phillips, O. M. (1984), On the response of short ocean wave components at a fixed wavenumber to ocean current variations, *J. Phys. Oceanogr.*, *14*, 1425–1433.

Phillips, O. M. (1985), Spectral and statistical properties of the equilibrium range in wind-generated gravity waves, *J. Fluid Mech.*, *156*, 505–531.

Plant, W. J. (1982), A relationship between wind stress and wave slope, *J. Geophys. Res.*, *87*, 1961–1967.

Plant, W. J. (1986), A two-scale model of short wind-generated waves and scatterometry, *J. Geophys. Res.*, *91*, 10,735–10,749.

Plant, W. J. (1997), A model for microwave Doppler sea return at high incident angles: Bragg scattering from bound, tilted waves, *J. Geophys. Res.*, *102*, 21,131–21,146.

Wentz, F. J. (1976), Cox and Munk's sea surface slope variance, *J. Geophys. Res.*, *81*, 1607–1608.

P. A. Hwang, Oceanography Division, Naval Research Laboratory, Building 1009, Room B151, Stennis Space Center, MS 39529, USA. (phwang@nrlssc.navy.mil)